

## Piezoelectric response of nanoscale $\text{PbTiO}_3$ in composite $\text{PbTiO}_3$ - $\text{CoFe}_2\text{O}_4$ epitaxial films

Zhuopeng Tan,<sup>1,a)</sup> Alexander L. Roytburd,<sup>1</sup> Igor Levin,<sup>2,a)</sup> Katyayani Seal,<sup>3</sup>  
 Brian J. Rodriguez,<sup>3</sup> Stephen Jesse,<sup>3</sup> Sergei Kalinin,<sup>3</sup> and Art Baddorf<sup>3</sup>

<sup>1</sup>*Department of Materials Science and Engineering, University of Maryland, College Park, Maryland 20742, USA*

<sup>2</sup>*Ceramics Division, National Institute of Standards and Technology, Gaithersburg, Maryland 20899, USA*

<sup>3</sup>*Center for Nanophase Materials Sciences, Oak Ridge National Laboratory, Oak Ridge, Tennessee 37831, USA*

(Received 28 June 2008; accepted 18 July 2008; published online 20 August 2008)

Piezoelectric properties of  $\text{PbTiO}_3$  in  $1/3\text{PbTiO}_3$ - $2/3\text{CoFe}_2\text{O}_4$  transverse epitaxial nanostructures on differently oriented  $\text{SrTiO}_3$  were analyzed using conventional and switching-spectroscopy piezoelectric force microscopy. The results confirmed that the individual  $\text{PbTiO}_3$  nanocolumns in the  $\text{CoFe}_2\text{O}_4$  matrix exhibit a detectable piezoelectric response regardless of substrate orientation. For the  $\{100\}$  and  $\{110\}$  orientations, a bias of  $\pm 10$  V produced ferroelectric domain switching; however, no switching was observed for the  $\{111\}$  films. Small values of piezoelectric constants  $d_{zz}^{(100)} \approx 11$  pm/V,  $d_{zz}^{(110)} \approx 5$  pm/V, and  $d_{zz}^{(111)} \approx 3$  pm/V are attributed to the weak intrinsic response of the nano- $\text{PbTiO}_3$  under strong mechanical and depolarizing-field constraints in the composite films. © 2008 American Institute of Physics. [DOI: 10.1063/1.2969038]

Fundamental understanding of a ferroelectric response in nanostructured materials is critical for their implementation in practical devices. Recently, multiple theoretical studies of polarization behavior in ferroelectric nanoparticles have been reported;<sup>1-4</sup> however, experimental verification of the proposed models and hypotheses is hindered by the lack of suitable samples and difficulties with nanoscale ferroelectric measurements. Epitaxial self-assembly of lattice-matched phases on matching single crystal substrates provides a viable approach for generating nanoscale ferroelectric features embedded in a nonferroelectric matrix. This approach has been used successfully to grow transversely modulated multiferroic nanostructures consisting of ferroelectric perovskite and ferrimagnetic spinel phases on single crystal  $\text{SrTiO}_3$ .<sup>5</sup> The morphology of constituent phases in these self-assembled nanostructures was effectively controlled using substrate orientation and phase fractions. For perovskite-spinel systems, nanorods of a perovskite phase in a spinel matrix have been obtained for the  $\text{PbTiO}_3$ - $\text{CoFe}_2\text{O}_4$  on  $\{110\}$  and  $\{111\}$   $\text{SrTiO}_3$  substrates, and for  $\text{BiFeO}_3$ - $\text{CoFe}_2\text{O}_4$  on  $\{111\}$   $\text{SrTiO}_3$ .

Several studies examined a ferroelectric response of the  $\{111\}$ -oriented  $\text{BiFeO}_3$ - $\text{CoFe}_2\text{O}_4$  films containing  $\text{BiFeO}_3$  nanorods in a  $\text{CoFe}_2\text{O}_4$  matrix.<sup>6</sup> The ferroelectric nature of individual  $\text{BiFeO}_3$  columns has been confirmed using piezoelectric force microscopy (PFM). The direction of spontaneous polarization in rhombohedral  $\text{BiFeO}_3$  coincides with the nanorod axis, thereby facilitating both piezoelectric and ferroelectric responses. The situation is significantly different for tetragonal perovskitelike phases, such as  $\text{BaTiO}_3$  and  $\text{PbTiO}_3$ , because, in the  $\{110\}$ - and  $\{111\}$ -oriented composite films, the  $\{001\}$  direction of spontaneous polarization is strongly inclined to the perovskite/spinel interfaces. No analysis of ferroelectric behavior in this kind of nanostruc-

tures has yet been reported. In the present study, we used both conventional PFM and switching-spectroscopy PFM (SS-PFM) to analyze the piezoelectric response of the  $\text{PbTiO}_3$  nanocolumns in  $1/3\text{PbTiO}_3$ - $2/3\text{CoFe}_2\text{O}_4$  self-assembled nanostructures on  $\{110\}$ - and  $\{111\}$ -oriented  $\text{SrTiO}_3$  substrates.<sup>7-9</sup> SS-PFM enables local piezoelectric measurements without electrodes thereby alleviating electrical leakage problems associated with a  $\text{CoFe}_2\text{O}_4$  matrix;<sup>10</sup> this leakage complicates direct measurements of a ferroelectric response in nanostructures having  $\text{CoFe}_2\text{O}_4$  as a majority phase.

$1/3\text{PbTiO}_3$ - $2/3\text{CoFe}_2\text{O}_4$  films were grown on  $\text{SrTiO}_3$  using pulsed laser deposition and a composite ceramic target, as described previously.<sup>6</sup> In all cases, film thicknesses were about 50 nm.  $\text{PbTiO}_3$  and  $\text{CoFe}_2\text{O}_4$  self-assemble during growth into epitaxial nanostructures having  $\text{PbTiO}_3/\text{CoFe}_2\text{O}_4$  interfaces approximately perpendicular to the film/substrate interface. Films grown on  $\{001\}$   $\text{SrTiO}_3$  contain  $\text{CoFe}_2\text{O}_4$  pillars surrounded by a continuous  $\text{PbTiO}_3$  matrix. In contrast, nanostructures grown on  $\{110\}$  and  $\{111\}$   $\text{SrTiO}_3$  contain nanocolumns of  $\text{PbTiO}_3$  distributed in  $\text{CoFe}_2\text{O}_4$ . X-ray diffraction, scanning electron microscopy (SEM) and transmission electron microscopy were used to assess the crystalline quality and phase morphologies. Detailed microscopy studies of phase morphologies in these films were reported previously.<sup>11</sup>

The SS-PFM was implemented using a commercial atomic force microscope (Asylum MFP3D) equipped with additional function generator and lock-in amplifier (DS 345 and SRS 830, Stanford Research Instruments) and an external signal generation, data acquisition system. The use of brand or trade names does not imply endorsement of the product by NIST.<sup>8</sup> Measurements were performed using Micromasch Au-Cr coated Si tips having a spring constant of 3 N/m. During the acquisition process, the tip was biased using electrical voltage  $V_{\text{tip}} = V_{\text{dc}} + V_{\text{ac}} \cos(\omega t)$  and the electromechanical response of the surface was detected as the first

<sup>a)</sup>Authors to whom correspondence should be addressed. Electronic addresses: zhuopeng@gmail.com and igor.levin@nist.gov.

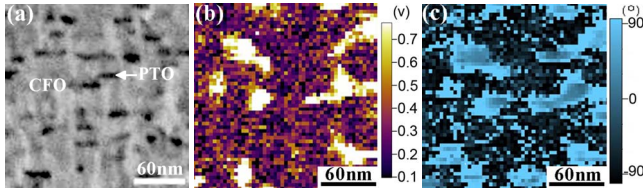


FIG. 1. (Color online) (a) SEM, (b) SS-PFM amplitude, and (c) phase images of the  $1/3\text{PbTiO}_3$ - $2/3\text{CoFe}_2\text{O}_4$  film on  $\{110\}$   $\text{SrTiO}_3$ . The SEM image reveals  $\text{PbTiO}_3$  platelets (dark contrast) having width of  $\approx 15$  nm dispersed in a  $\text{CoFe}_2\text{O}_4$  matrix. The  $\text{PbTiO}_3$  columns appear bright in the PFM amplitude image; the column shape is somewhat blurred and distorted (compared to SEM) because of the tip and sample geometries.

harmonic component ( $A_{1\omega}$ ) of bias-induced tip deflection,  $A = A_0 + A_{1\omega} \cos(\omega t + \varphi)$ . The measurements were conducted using a step (pixel) size of 6 nm. At each point, the piezoelectric response was recorded as a function of the tip bias.

SEM images of the  $\{110\}$  film [Fig. 1(a)] reveal platelet-like columns of  $\text{PbTiO}_3$  embedded in  $\text{CoFe}_2\text{O}_4$ ; the lateral size of these columns is  $\approx 15$  nm. A SS-PFM map [Fig. 2(a)] of piezoelectric response, recorded on the same film, reveals nanoscale active areas (dark) that can be readily correlated with the  $\text{PbTiO}_3$  columns as seen in the SEM images; as expected, no significant piezoelectric response is detected from the  $\text{CoFe}_2\text{O}_4$  matrix. SS-PFM provides both PFM displacement amplitude [Fig. 1(b)] and phase [Fig. 1(c)] information for each pixel in the map ( $60 \times 60$  pixels).

Figures 2(b)–2(f) summarize individual displacement and phase loops for points 1 to 3 in Fig. 2(a). The butterfly-shaped amplitude loop [Fig. 2(d)] recorded from point 3, which is located within the  $\text{PbTiO}_3$  column, provides information on the magnitude of the piezoelectric response, whereas the phase change of  $\approx 180^\circ$  as seen in the corresponding phase loop [Fig. 2(e)] confirms ferroelectric domain switching. Clearly, a dc bias of 10 V was insufficient to saturate the piezoelectric response. The amplitude and phase data were combined to generate a piezoelectric loop in Fig. 2(f). A change in the sign of the tip deflection in this combined loop indicates domain switching whereas the absolute

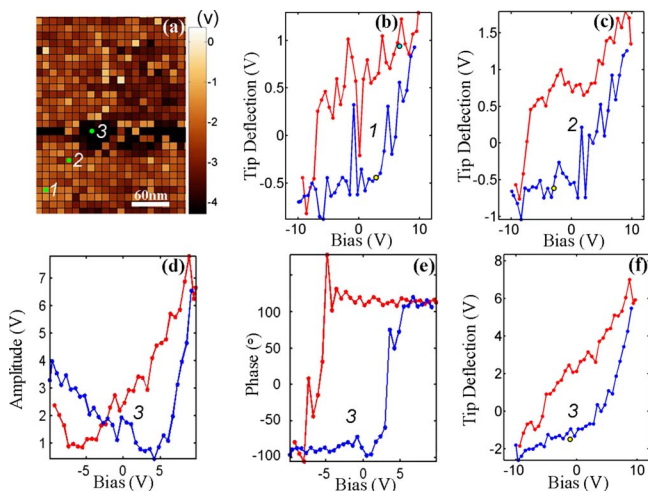


FIG. 2. (Color online) (a) A map of switchable polarization for the  $\{110\}$   $1/3\text{PbTiO}_3$ - $2/3\text{CoFe}_2\text{O}_4$  film. Dark areas correspond to  $\text{PbTiO}_3$ . (b) and (c) are piezoelectric hysteresis loops at points 1 and 2, respectively. (d) Amplitude of the piezoelectric response at point 3. (e) Phase of the piezoelectric response at point 3. (f) Combined amplitude/phase piezoelectric hysteresis loop at point 3.

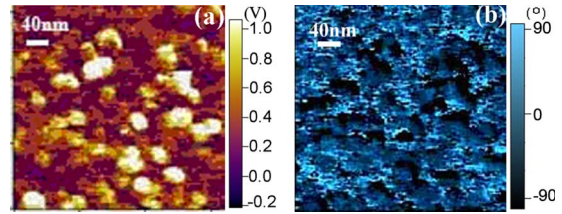


FIG. 3. (Color online) (a) Conventional-PFM amplitude and (b) phase images of the  $\{111\}$   $1/3\text{PbTiO}_3$ - $2/3\text{CoFe}_2\text{O}_4$  film.  $\text{PbTiO}_3$  columns appear bright in the amplitude image.

values of deflection reflect the magnitude of a piezoelectric response. The area within the piezoelectric hysteresis loop corresponds to the work on domain switching.

Piezoelectric response decays markedly as the tip is moved away from  $\text{PbTiO}_3$  into  $\text{CoFe}_2\text{O}_4$  as can be seen from the amplitude loops for points 1–3. Based on previous experience, the tip diameter is  $\approx 60$  nm which is comparable to the typical distances separating individual  $\text{PbTiO}_3$  columns. Thus, a nonzero response is sensed even for locations well within the  $\text{CoFe}_2\text{O}_4$  matrix because the tip still interacts with  $\text{PbTiO}_3$ .

SEM images of the  $\{111\}$ -oriented nanostructures highlight triangular-shaped  $\text{PbTiO}_3$  columns (lateral size  $\approx 30$  nm) dispersed in  $\text{CoFe}_2\text{O}_4$ . Conventional PFM of the same film yields bright regions which exhibit a significant piezoelectric response [Fig. 3(a)] and a phase angle different from that of the surrounding material (dark). Size and number density of these regions suggest them to represent nanocolumns of  $\text{PbTiO}_3$ . Despite evident piezoelectric activity of the  $\langle 111 \rangle$ -aligned  $\text{PbTiO}_3$  columns, no domain switching could be observed upon changing the bias from  $-10$  to  $10$  V. SS-PFM measurements on the  $\{001\}$ -oriented film (Fig. 4), used as a reference, revealed a strong piezoelectric response from the  $\text{PbTiO}_3$  regions with a clearly identifiable domain switching.

Accurate calculations of the piezoelectric coefficients from the SS-PFM measurements are difficult because of the inhomogeneous electric/strain fields under the tip. Nevertheless, rough estimates of  $d_{zz}$  can be obtained as  $d_{zz} = \text{displacement}/\text{bias}$ , assuming similar spatial distributions for both electric and strain fields. Our SS-PFM measurements yield  $d_{zz}^{(100)} \approx 11$  pm/V,  $d_{zz}^{(110)} \approx 5$  pm/V and  $d_{zz}^{(111)} \approx 3$  pm/V (superscript indicates a crystallographic orientation of the film). These  $d_{zz}$  values are approximately five times smaller than those measured for the  $1/3\text{PbTiO}_3$ - $2/3\text{CoFe}_2\text{O}_4$  films which contained  $\text{CoFe}_2\text{O}_4$  columns in the  $\text{PbTiO}_3$  matrix.<sup>12</sup> The polydomain nature of  $\text{PbTiO}_3$  in the composite films<sup>7</sup> with the  $c$ -domain fraction of about 50% is expected to reduce significantly the spontaneous po-

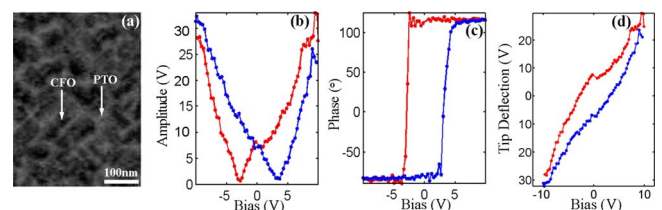


FIG. 4. (Color online) (a) SEM image of the  $\{100\}$   $1/3\text{PbTiO}_3$ - $2/3\text{CoFe}_2\text{O}_4$  film. (b) Amplitude, (c) phase, and (d) combined signal for a piezoelectric response from the  $\text{PbTiO}_3$  region. The ferroelectric domain switching is clearly observed in the phase loop.

larization compared to its single-domain value. The polarization is further diminished by the dissolution in Fe in  $\text{PbTiO}_3$  as manifested in the reduced strain-free tetragonality of this phase in the nanostructures.<sup>13</sup> Therefore, an *intrinsic* piezoelectric response of the {001} film is expected to be considerably weaker than 50 pm/V previously measured on the {001}  $1/3\text{CoFe}_2\text{O}_4-2/3\text{PbTiO}_3$  nanostructures using electrodes.<sup>12</sup> This relatively strong response (compared to the value of 79 pm/V for a freestanding  $\text{PbTiO}_3$  film) (Ref. 14) can be explained only assuming a substantial *extrinsic* piezoelectric effect associated with the  $90^\circ$ -domain wall movement. The feasibility of this mechanism is supported by the complete reversibility of the  $90^\circ$ -domain structures upon heating/cooling the composite films across the Curie temperature.<sup>13</sup> In contrast to electrode-based PFM measurements which ensure a uniform electric field in the film under the top electrode, the highly localized dc field applied during the SS-PFM measurements appears insufficient to produce any significant movement of the  $90^\circ$  domains in the nano-scale  $\text{PbTiO}_3$  features. Thus, the  $d_{zz}$  values estimated from the SS-PFM measurements likely reflect a weak intrinsic piezoelectric response of the nano- $\text{PbTiO}_3$  under the mechanical and depolarizing-field constraints imposed by the  $\text{CoFe}_2\text{O}_4$  phase.

- <sup>1</sup>I. Naumov, L. Bellaiche, and H. X. Fu, *Nature (London)* **432**, 737 (2004).
- <sup>2</sup>I. Ponomareva, I. Naumov, I. Kornev, H. Fu, and L. Bellaiche, *Curr. Opin. Solid State Mater. Sci.* **9**, 114 (2005).
- <sup>3</sup>E. K. Akdogan and A. Safari, *J. Appl. Phys.* **101**, 064114 (2007).
- <sup>4</sup>J. Slutsker, A. Artemev, and A. L. Roytburd, *Phys. Rev. Lett.* **100**, 087602 (2008).
- <sup>5</sup>H. Zheng, J. Wang, S. E. Lofland, Z. Ma, L. Mohaddes-Ardabili, T. Zhao, L. Salamanca-Riba, S. R. Shinde, S. B. Ogale, F. Bai, D. Viehland, Y. Jia, D. G. Schlom, M. Wuttig, A. L. Roytburd, and R. Ramesh, *Science* **303**, 661 (2004).
- <sup>6</sup>H. Zheng, Q. Zhan, F. Zavaliche, M. Sherburne, F. I. Straub, M. P. Cruz, L. Q. Chen, U. Dahmen, and R. Ramesh, *Nano Lett.* **6**, 1401 (2006).
- <sup>7</sup>S. V. Kalinin, A. Rar, and S. Jesse, *IEEE Trans. Ultrason. Ferroelectr. Freq. Control* **53**, 2226 (2006).
- <sup>8</sup>S. Jesse, A. P. Baddorf, and S. V. Kalinin, *Appl. Phys. Lett.* **88**, 062908 (2006).
- <sup>9</sup>B. J. Rodriguez, S. Jesse, A. P. Baddorf, T. Zhao, Y. H. Chu, R. Ramesh, E. A. Eliseev, A. N. Morozovska, and S. V. Kalinin, *Nanotechnology* **18**, 405701 (2007).
- <sup>10</sup>Y. Yamazaki and M. Satou, *Jpn. J. Appl. Phys.* **12**, 998 (1973).
- <sup>11</sup>I. Levin, J. Li, J. Slutsker, and A. L. Roytburd, *Adv. Mater. (Weinheim, Ger.)* **18**, 2044 (2006).
- <sup>12</sup>J. Li, I. Levin, J. Slutsker, V. Provenzano, P. K. Schenck, R. Ramesh, J. Ouyang, and A. L. Roytburd, *Appl. Phys. Lett.* **87**, 072909 (2005).
- <sup>13</sup>I. Levin, J. Li, Z. Tan, J. Slutsker, and A. L. Roytburd, *Appl. Phys. Lett.* **91**, 062912 (2007).
- <sup>14</sup>J. Ouyang, R. Ramesh, and A. L. Roytburd, *Adv. Eng. Mater.* **7**, 229 (2005).